

Learning from the Barn Owl Auditory System: A Bio-Inspired Localization Hardware Architecture

Enrico Heinrich and Ralf Joost and Ralf Salomon
Faculty of Computer Science and Electrical Engineering
University of Rostock
18051 Rostock, Germany

e-mail: {enrico.heinrich,ralf.joost,ralf.salomon}@uni-rostock.de

Abstract—Normally, research on evolutionary computation applies its algorithms to the solution or optimization of some technical or mathematical problems. But for some technical tasks, such as localization, nature seem to provides optimal solutions. This paper discusses how the barn owl auditory system can be conceptually realized on a digital system, such as a field-programmable gate array. This adapted system yields a time resolution as small as 20 ps, even though it is clocked at only 85 MHz, which corresponds to a duty cycle of about 12 ns. The system achieves this result by copying the natural role model’s core principles, i.e., employing a large number of simple, slowly operating processing elements, which are all connected to two passive wires, which induce only a very small additional time delay; these properties are the result of a natural evolutionary process that has taken millions of years.

Index Terms—natural evolution, bionic, barn owl, high precision localization.

I. INTRODUCTION

The application of evolutionary algorithms to practically relevant problems is an important process in many respects: for example, it allows for the verification of theoretical analyzes, it provides performance figures on standard benchmark tests, and it offers (optimal) solutions to mathematical as well as engineering problems. For obvious reasons, the vast majority of all these “practical experiments” are performed in computer simulations (only): the application of certain variation operators, such as mutation and recombination, the transformation from genotype to phenotype, and the actual fitness calculation can often be done very easily in software.

But the literature also provides some truly real-world applications, such as the optimization of the “pipe-elbow” [1], the optimization of the two-phase nozzle [1], [2], or the evolution of adaptive controllers for autonomous agents [3], [4], [5]. In spite of their successes, these applications also indicate that practical real-world experimentation is limited to a small number of (representative) test cases: the time to manufacture and to evaluate all offspring is *the* limiting factor. Therefore, such research often employs some workarounds in order to make the required experimentation time manageable.

The currently observable technology gap, in a sense that physical objects can be “produced” in short (instant) time from a given genotype, suggests that at least in the near future, the application of evolutionary algorithms will still be focusing on mathematical and/or software simulations, which may be

considered an unfortunate restriction. However, the scientific discipline called *bionic* [6], [7], [8] argues that in many cases, the application of evolutionary or other optimization algorithms is not always required, since nature already provides optimal or at least very inspiring solutions [1]. That means that bionic does not try to optimize a technical draft version but rather transfers a natural solution, architecture, or method to technical problems of interest.

Localization [9], [10] is one of those problems that are relevant in both domains nature and engineering. For example, a predator has to localize its prey, a smart infrastructure has to determine the position of a laptop. Localization is a process that derives new, so-far unknown points from a set of given reference points by evaluating angles and/or distances. Section II briefly describes the standard localization setup, and explains how the position can be derived from the time-difference-of-arrival.

Localization by determining certain angles is quite omnipresent in nature. Among all the natural solutions offered, the barn owl is an impressive evolutionary result: its auditory system yields an angular resolution that is about one order of magnitude better than the *processing speed* of its neurons would allow. Since it serves as the role model of the localization approach proposed in this paper, the barn owl auditory system is briefly described in Section III.

Section IV describes how the barn owl auditory system can be implemented on a digital circuit, known as a field-programmable gate array (FPGA). This circuit consists of a very large number of logic elements that can be arbitrarily interconnected according to the programmers desire. Because of its internal structure, this localization system is called exclusively-ored counter array, or X-ORCA for short.

The X-ORCA architecture has already been implemented as a first prototype, which is briefly discussed in Section V. The implementation was done on a standard, low-cost FPGA, which is clocked at about 85 MHz (with a duty cycle of about 12 ns) and which charges about 50 USD¹. This prototype has been used in some practical experiments, which are summarized in Section VI. Its main result is that the X-ORCA system yields a resolution as small as 20 ps, which is about

¹A complete development board, which features all the required components and interfaces, charges about 500 USD. However, such a board is required only during research and development, not in a running system.

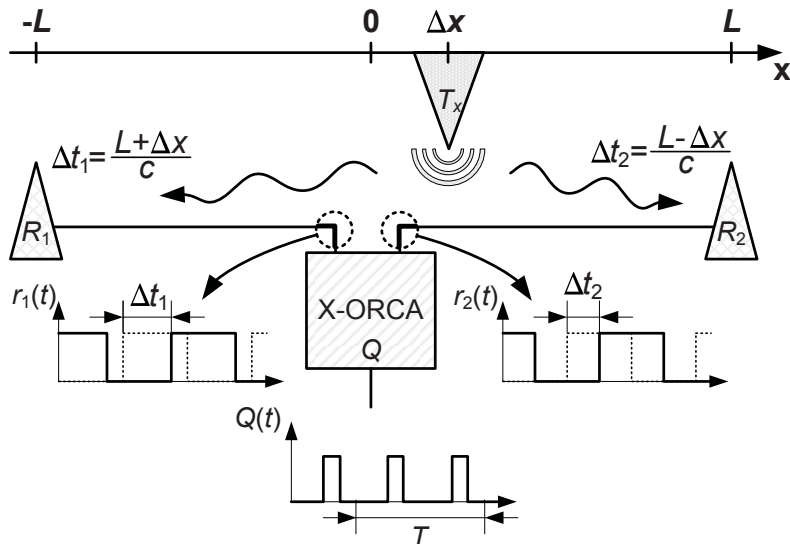


Fig. 1. This paper assumes a standard setup, which is simplified to one dimension here. The two receivers read the transmitter's signals after they have traveled the two distances $L + \Delta x$ and $L - \Delta x$. Thus, the time difference $\Delta t = t_1 - t_2 = 2\Delta x/c$ is a result of the transmitter's off-center position Δx . The system indirectly determines $\Delta t = \Delta\varphi/(2\pi f)$ by estimating the phase shift $\Delta\varphi$ between the two incoming signals $r_1(t)$ and $r_2(t)$.

three orders of magnitude better than the system clock's duty cycle of about 12 ns. Finally, Section VII concludes this paper with a brief discussion.

In summary: rather than evolving a technical system by means of some artificial evolutionary algorithms, this paper reports on a technical realization of a (localization) concept that has been evolved by natural evolution over millions of years. In other words, the described technical achievements are not due to the authors' ingeniousness but not rather due nature's role model.

II. PROBLEM DESCRIPTION: LOCALIZATION

Generally, localization systems come in two flavors: (1) a set of receivers (passive infrastructure) determines the location of an active sender, or (2) a passive receiver derives its own position from the signals emitted by a set of active transmitters. In accordance with the barn owl (and almost all other animals), this paper assumes the first setup.

For educational purpose and for the ease of development, this paper assumes a one-dimensional setup as is illustrated in Figure 1; an extension to a two or three-dimensional setup can be simply realized by duplicating or tripling the one-dimensional setup, and is thus not further discussed in this paper.

In a one-dimensional setup, an active transmitter T emits a (sound or electromagnetic) signal $s(t) = A\sin(2\pi f(t - t_0))$ with frequency f , amplitude A , and time offset t_0 . After traveling the two distances $L + \Delta x$ and $L - \Delta x$, the signals arrive at the two receivers R_1 and R_2 . Since this traveling happens with a finite speed c , it arrives at the receivers after the time delays $\Delta t_1 = (L + \Delta x)/c$ and $\Delta t_2 = (L - \Delta x)/c$.

In order to further digitally process the received signals, all receivers generally employ an amplifier and a Schmitt trigger, which converts any input signal into a rectangular one.

Therefore the two receivers provide the rectangular signals $r_1(t - t_0 - \Delta t_1)$ and $r_2(t - t_0 - \Delta t_2)$, with Δt_1 and Δt_2 denoting the aforementioned time delays that are due to the finite signal traveling speed.

Finally, the localization system has to determine the time difference $\Delta t = \Delta t_1 - \Delta t_2$ between the two received signals $r_1(t - t_0 - \Delta t_1)$ and $r_2(t - t_0 - \Delta t_2)$. If the localization system knows the signal frequency f , it can accomplish this in an indirect way $\Delta t = \Delta\varphi/(2\pi f)$ by determining the phase shift $\Delta\varphi$ between the two signals.

It might be, though, that both the physical setup and the localization system have further internal delays, such as switches, cables of different lengths, repeaters, and further logical gates. However, these internal delays can all be omitted, since they can be easily eliminated in a proper calibration process.

Localization by measuring the time-difference-of-arrival becomes particularly challenging, if the system is based on electromagnetic signals, which travel with the speed of light $c \approx 3 \cdot 10^8$ m/s. For example, an electromagnetic signals travels 1 cm in approximately 33 ps.

III. BACKGROUND: THE BARN OWL AUDITORY SYSTEM

Figure 2 illustrates that the barn owl localization system consists of two ears, two axonal delay lines, and a decent number of neurons. All the neurons are connected to both axonal delay lines and operate as coincidence detectors. The activity of such a coincidence detector increases as the two input signals get more and more similar; the neuron's activity is maximal, if both inputs are equivalent.

In case the barn owl perceives a sound signal (of a potential prey), the neuronal activity of the two ears are forwarded to the nucleus laminaris via the two axonal delay lines. Due to these delay lines, the signals are further delayed as they travel

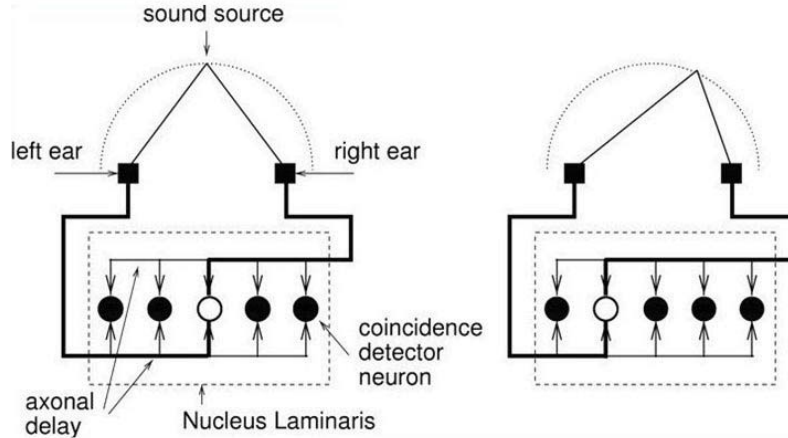


Fig. 2. The barn owl auditory system (nucleus laminaris) consists of a decent number of neurons, which all operate as coincidence detectors and which are all connected to axonal delay lines. Depending on the location of the sound source, all the neurons exhibit different activities.

along these axons. That means that these internal delays add to the external delays, which are due to the sound source's location and the finite speed of the signal. Consequently, the neurons of the nucleus laminaris form an activation pattern that is unique to the sound source's location (angle).

Figure 2 shows two examples. On the left-hand-side, the sound source is in the center, and thus the center neuron responds maximally. In the example on the right-hand-side, the sound source is moved to the right. Consequently, the neuron with the highest activity is on the left, where the internal delays compensate for the external asymmetry.

Because of its internal architecture, the barn owl auditory system has an astonishing property: taking into account only the processing speed of the neurons, the system would be able to achieve a localization accuracy of as poor as 30° . However, the barn owl achieves an accuracy as good as 2° . This is mainly due to the following properties: (1) the axonal delay is much smaller than the processing time within a neuron, and (2) due to their massively parallel processing, all neurons exhibit a different response, which lead to significant response changes even for small changes of the sound source's location. For further details, the interested reader is referred to the pertinent literature [11].

IV. THE X-ORCA LOCALIZATION SYSTEM

This section proposes a localization system called X-ORCA, which is an acronym for XOR-ed counter array. On an abstract level, this system has quite the same architecture as the barn owl auditory systems. It consists of two inputs (the two ears), two regular wires (the two axonal delays), and quite a number of coincidence detectors (the neurons).

The description of the (digital) coincidence detectors requires a little more care. First of all, simple logic gates cannot be operating as coincidence detectors. Then, "coincidence" of two signals can be interpreted such that there is no difference between them; in other words, they are identical at all times.

The difference of two signals is easy to detect, a simple XOR gates does the job. An XOR gate delivers a logical one, if either of the two inputs has a logical one but not both. Thus, the proportion of a logical one with respect to a logical zero at the output of an XOR gate expresses the phase shift φ between the two inputs (see, also, Section II).

With an XOR gate as the combiner of the two inputs, the task is to measure the average duration of the logical ones at its output. This can be achieved with the circuitry illustrated in Figure 3. The output of the XOR gate is connected to the enable input of a simple counter. This counter increases its value, if at the clock signal (actually the transition from a logical zero to a logical one), the enable input is activated. Thus, the counter value is proportional to the timely proportion of logical ones at the XOR gate's output and the total number of clock cycles. This value is thus proportional to the phase shift $\Delta\varphi$ between both input signals.

For example, let us assume an input signal with a frequency of $f = 100 \text{ MHz}$ and a phase shift of $\Delta\varphi = \pi/4 = 45^\circ$.

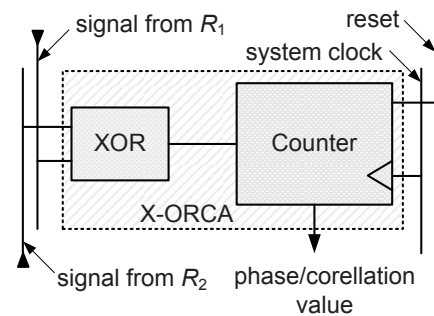


Fig. 3. The combination of a simple XOR gate and a subsequent counter is able to operate as a coincidence detector. The counter value is proportional to the proportion of logical ones at the XOR gate's output and the total number of clock cycles. The counter value is thus proportional to the phase shift $\Delta\varphi$ between both input signals.

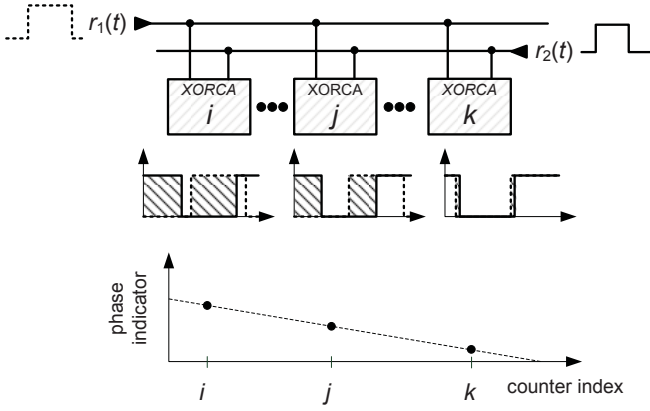


Fig. 4. X-ORCA places all phase detectors along two reciprocal (anti-parallel) “delay” wires w_1 and w_2 on which the two signals $r_1(t)$ and $r_2(t)$ travel with approximately two third of the speed of light $c_w \approx 2/3c$. Because the two wires w_1 and w_2 are *reciprocal*, all phase detectors have different internal delays τ_i .

Then, if the counter is clocked at a rate of 10GHz over a signal’s period $T = 1/(100 \text{ MHz}) = 10 \text{ ns}$, the counter will assume a value of $v = 25$. In this example, all the given numbers, particularly the chosen frequencies, are for educational purposes only, and may not be realistic in a specific implementation.

As has already been seen in the barn owl auditory system, X-ORCA also employs a large number of coincidence detectors (see Figure 4), which are all connected to two reciprocal (anti-parallel) “delay” wires w_1 and w_2 on which the two signals $r_1(t)$ and $r_2(t)$ travel with approximately two third of the speed of light $c_w \approx 2/3c$.

The mode of operation of the X-ORCA system is quite identical to that of the barn owl. Let us start with the coincidence detector (neurons) at which the two inputs match, i.e., both inputs have a vanishing phase shift $\varphi = 0$. Then, due to the “delays” along the two wires w_1 and w_2 , the coincidence detectors to the right and left observe non-matching inputs, i.e., non-vanishing phase shifts $\varphi \neq 0$. If the delay wires cause a time delay δ between two coincidence detectors, then these detectors observe a total time shift of 2δ . That is, the duration of a logical one is also increased or decrease by 2δ .

Normally, the time difference 2δ is much smaller than the duty cycle of the counter, and would thus not have any effect. However, if sampling over a sufficiently long time span, this tiny time delay will eventually affect the *final* counter value.

V. THE FIRST PROTOTYPE

The first X-ORCA prototype was implemented on an Altera Cyclone II FPGA [12]. This device offers 33,216 logic elements and can only be clocked at about 85 MHz. The chosen FPGA *development board* is a low-cost device that charges about 500 USD.

On the top-level view, the X-ORCA prototype consists of 140 phase detectors, a common data bus, a Nios II soft core processor [13], and a system PLL that runs at 85 MHz.

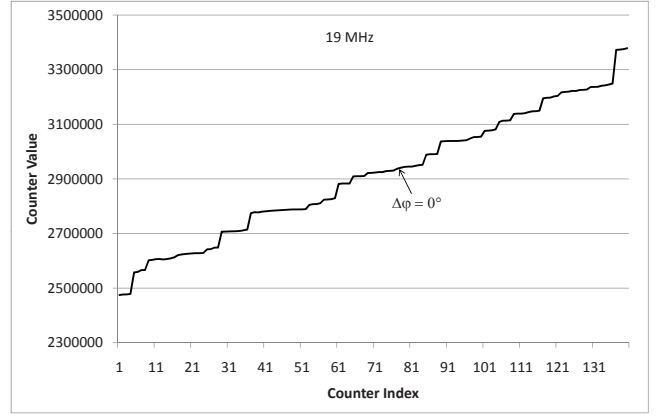


Fig. 5. The figure shows the counter values v_i of $n = 140$ phase detectors when fed with two 19 MHz signals with zero phase shift $\Delta\varphi = 0$.

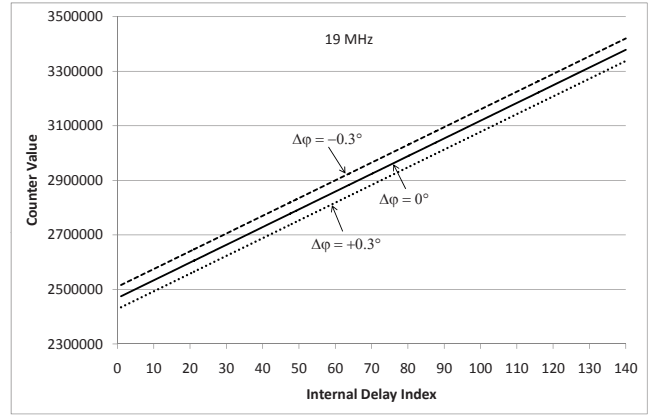


Fig. 6. The figure shows the derived counter values v_i of $n = 140$ phase detectors when fed with two 19 MHz signals with zero phase shift $\Delta\varphi = 0$ (solid line), with phase shift $\Delta\varphi \approx -0.3^\circ$ (dashed line), and with phase shift $\Delta\varphi \approx +0.3^\circ$ (dotted line).

The Nios II processor manages all the counters of the phase detectors, and reports the results via an interface to a PC.

Due to the limited laboratory equipment, the transmitter is realized as a simple function generator that emits a sinusoidal signal. In order to focus on the core system, wireless communication capabilities were not employed; rather, the prototype is connected to the function generator via a regular wire as well as a line stretcher [14]. Such a line stretcher can be extended or shorted, and can thus change the signal propagation time accordingly.

It should be noted, though, that X-ORCA’s internal “delay wires” w_1 and w_2 are realized as pure passive internal wires, connecting the device’s logic elements, as previously announced in Section IV.

VI. RESULTS

Figures 5-10 summarize the experimental results that were achieved by the first X-ORCA prototype under different configurations. Unless otherwise stated, these figures present the

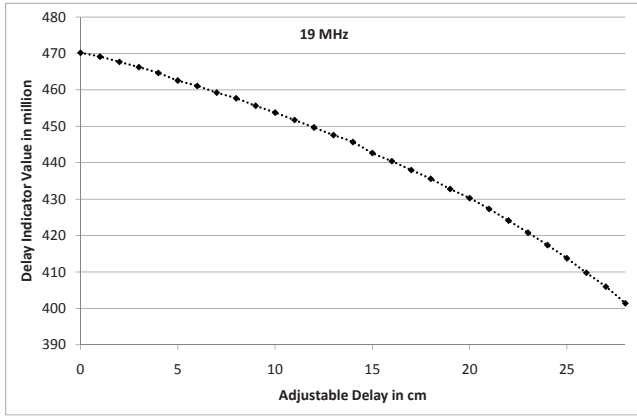


Fig. 7. The figure shows the delay value indicator resulting from adjustable delay line lengths when fed with two 19 MHz signals.

counter values v_i of $n = 140$ different phase detectors, which were clocked at a rate of 85 MHz.

Figure 5 shows the behavior of the X-ORCA architecture when using the external 19 MHz localization signal. In this experiment, one of the connections from the function generator to the input pad of the development board was established by a line stretcher [14], whereas the other one was made of a regular copper wire. Figure 5 shows the values v_i of the $n = 140$ counters, which were still clocked at 85 MHz over a measurement period of 10,000,000 ticks.

In addition, Figure 5 reveals some technological FPGA internals that might be already known to the expert reader: neighboring logic elements do not necessarily have equivalent technical characteristics and are not interconnected by a regular wire grid. As a consequence, the counter values v_i and v_{i+1} of two neighboring phase detectors do not steadily increase or decrease, which makes the curve look a bit rough. This effect can be compensated. Each counter has a unique and constant internal delay, therefore, the counter values v_i can be plotted

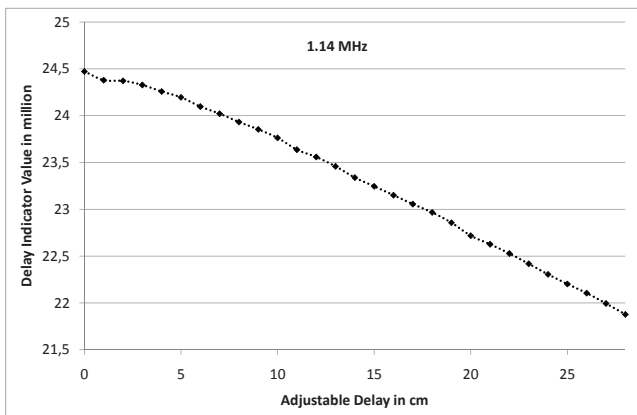


Fig. 8. The figure shows the delay value indicator when employing two 1.14 MHz localization signals. The data points results from varying length of the employed line stretcher.

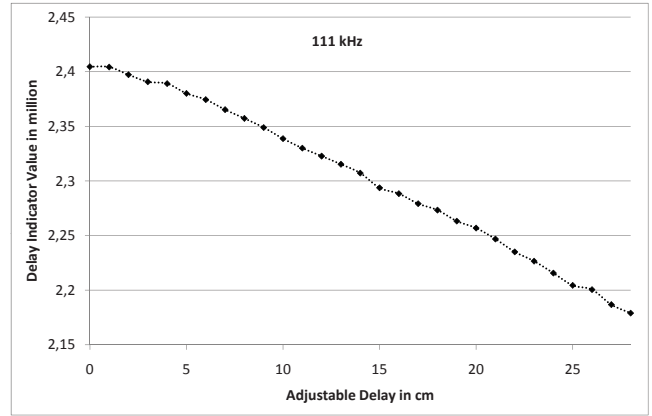


Fig. 9. The figure shows the delay value indicator when employing two 111 kHz localization signals. The data points results from varying length of the employed line stretcher.

over the internal delay τ_i that results in a flat curve as shown in Figure 6.

The three graphs in Figure 6 refer to a phase shift of $\Delta\varphi \in \{-0.3^\circ, 0, +0.3^\circ\}$, which corresponds to time delays $\Delta t \in \{-0.02 \text{ ns}, 0 \text{ ns}, +0.02 \text{ ns}\}$. It should be noted that the graph of this figure appears as a straight line, since the internal time delays τ_i span much less than an entire period of the 19 MHz signal.

Figure 7 presents a different view of Figure 6: In the graph, every dot represents the sum $v_{\text{tot}} = \sum_i v_i$ of all $n = 140$ counter values v_i ; that is, an entire graph of Figure 6 is collapsed into one single dot. The graph shows 29 measurements in which the line stretcher was extended by 1 cm step by step. It can be seen that a length difference of $\Delta x = 1 \text{ cm}$ decreases v_{tot} by about 20 million. This result suggests that with a localization of 19 MHz, X-ORCA is able to detect a length difference of about $\Delta x = 1 \text{ mm}$, which equals a time resolution of about 0.02 ns.

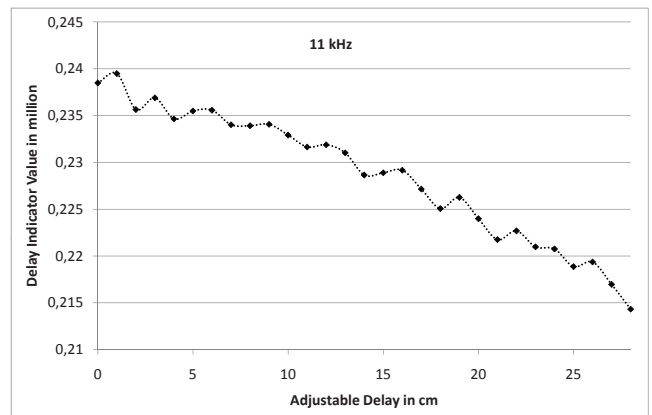


Fig. 10. The figure shows the delay value indicator when employing two 11 kHz localization signals. The data points results from varying length of the employed line stretcher.

The second focus of the practical experiments was to explore the lower limit of the normalized time delay $\Delta t/f$. To this end, the prototype was exposed to two localization signals with varying time delays. The localization frequencies were set to $f \in \{1.14 \text{ MHz}, 111 \text{ kHz}, 11 \text{ kHz}\}$. The results are plotted in Figures 8-10.

All three figures show the very same qualitative behavior. The only difference is the absolute value of the delay value indicator: a decrease of the localization frequency by a factor of 10 leads to a reduction of the delay value indicator by the very same amount; with the identical time delay Δt the phase shift is only a tenth, if the frequency is also just a tenth.

VII. DISCUSSION

This paper has argued that it is not always required to utilize (artificial) evolutionary algorithms in order to solve open technical problems. For some problems, nature has already evolved optimal solutions. In that case, the natural solution has to be transferred to the technical application at hand. This process is also known as *bionic*.

As an example, this paper has analyzed the barn owl auditory system, since its resolution is much better than the processing speed of the neurons would allow. The barn owl achieves its impressive resolution by (1) employing a large number of coincidence detectors, which are (2) all connected to two passive axonal delay lines.

Then, this paper has described a digital implementation that employs all the relevant architectural concepts of the barn owl auditory system. The practical experiments show that this system achieves a resolution of about 20 ps, even though the system is clocked at 85 MHz, which corresponds to a duty cycle of about 12 ns. It might be noted that during 20 ps, an electromagnetic signal is able to travel a distance as short as approximately 6 mm. As has been already mentioned, these performance figures are not the result of the application of evolutionary algorithm in a laboratory setting, but rather due to natural evolution over millions of years.

Future research will be mainly devoted to three different avenues. The first step will be devoted to both an improved resolution and an extended effective range of operation. Because of the processing structures in higher level areas in the barn owl auditory system, the barn owl has equally distribute its phase detectors along the nucleus laminaris. An FPGA, however, has much better computational capabilities: the evaluation hard-/software can employ arbitrarily complex equations. To this end, an on-chip evolutionary process will be implemented. This process genetically code the placement of all the phase detectors. The fitness evaluation will consequently incorporate the aforementioned properties, i.e., resolution and effective range, as well as the number of employed phase detectors. The evolutionary process itself will be operate as usual: it will maintain a small number of genomes that are manipulated by standard evolutionary variation operators and evaluated by a proper fitness function.

The second research option will be exploring the system's limits by utilizing mproved laboratory equipment. Finally, the

third option of future research will devoted to the integration of wireless communication modules. The best option for that approach seems to be the utilization of a software-defined radio module, such as the Universal Software Radio Peripheral 2 (USRP2) [15]. Finally, future research will port the first prototype onto more state-of-the-art development boards, such as an Altera Stratix V FPGA [16].

ACKNOWLEDGEMENTS

The authors gratefully thank Volker Kühn and Sebastian Vorköper for their helpful discussions. This work was supported in part by the DFG graduate school 1424. Special thanks are due to Matthias Hinkfoth for valuable comments on draft versions of the paper.

REFERENCES

- [1] I. Rechenberg, *Evolutionsstrategie : Optimierung technischer Systeme nach Prinzipien der biologischen Evolution*. Stuttgart: Frommann-Holzboog, 1973.
- [2] J. Klockgether and H. P. Schwefel, "Two-phase nozzle and hollow-core jet experiments," in *Proceedings of the 11th Symposium on Engineering Aspects of MHD*. California Institute of Technology, 1970, pp. 141–148.
- [3] I. Harvey, P. Husbands, D. Cliff, A. Thompson, and N. Jakobi, "Evolutionary robotics: the sussex approach," in *Robotics and Autonomous Systems, Special Issues on "Practice and Future of Autonomous Agents"*, R. Pfeifer and R. B. (eds.), Eds., 1996.
- [4] D. Floreano and F. Mondada, "Evolution of homing navigation in a real mobile robot," in *IEEE Transactions on Systems, Man, and Cybernetics-Part B*, vol. 26, no. 3, June 1996.
- [5] R. Salomon, "Evolving receptive-field controllers for mobile robots," in *Applied Intelligence*. Kluwer, 2002, pp. 89–100.
- [6] I. Rechenberg, *Evolutionsstrategie '94*. Stuttgart: Frommann-Holzboog, 1994.
- [7] G. K. Hung, *Biomedical Engineering Principles Of The Bionic Man*. World Scientific Publishing Company, 2010.
- [8] S. Perrowitz, *Digital People: From Bionic Humans to Androids*. Joseph Henry Press, 2005.
- [9] P. Misra and P. Enge, "Global positioning system: Signals, measurements, and performance," in *2nd Edition, Ganga-Jamuna Press*, 2006.
- [10] S. Knauth, C. Jost, and A. Klapproth, "iloc: a localisation system for visitor tracking & guidance," in *Proceedings of the 7th IEEE International Conference on Industrial Informatics 2009 (INDIN 2009)*, 2009, pp. 262–266.
- [11] R. Kempter, W. Gerstner, and J. L. van Hemmen, "Temporal coding in the sub-millisecond range: Model of barn owl auditory pathway," *Advances in Neural Information Processing Systems*, vol. 8, pp. 124–130, 1996.
- [12] *Nios Development Board Cyclone II Edition Reference Manual*, Altera Corp., San Jose, CA, 2007, altera Document MNLN051805-1.3.
- [13] *Nios II Processor Reference Handbook*, Altera Corp., San Jose, CA, 2007, altera Document NII5V1-7.2.
- [14] *Microlab: "Line Stretchers, SR series"*, Datasheed, Microlab Company, 2008.
- [15] Ettus Research LLC, <http://www.ettus.com>.
- [16] *Stratix V Device Handbook*, Altera Corp., San Jose, CA, 2010, altera Document SV5V1-1.0.